Multilevel Transport Solution of LWR Reactor Cores

International Conference on Reactor Physics, Nuclear Power: A Sustainable Resource

Jose Ignacio Marquez Damian
Cassiano R. E. de Oliveira
HyeongKae Park

September 2008

Idaho National
Laboratory

Multilevel transport solution of LWR reactor cores

Jose Ignacio Marquez Damian[*,a], Cassiano R.E. de Oliveira[b],
HyeongKae Park[c]

[a] *Centro Atomico Bariloche, S.C. de Bariloche, Argentina*
[b] *University of New Mexico, Albuquerque, USA*
[c] *Idaho National Laboratory, Idaho Falls, USA*

Abstract

This work presents a multilevel approach for the solution of the transport equation in typical LWR assemblies and core configurations. It is based on the second-order, even-parity formulation of the transport equation, which is solved within the framework provided by the finite element-spherical harmonics code EVENT. The performance of the new solver has been compared with that of the standard conjugate gradient solver for diffusion and transport problems on structured and unstructured grids. Numerical results demonstrate the potential of the multilevel scheme for realistic reactor calculations.

1. Introduction

Nuclear reactor design requires the calculation of integral core parameters, power and neutron flux profiles. In the deterministic transport approach, these physical parameters are obtained by solving the linear neutron transport equation over the domain representing the reactor core. In order to represent the fine spatial structure of the reactor core, typically a very small spatial mesh size must be used which can lead to substantial computational effort both in terms of storage and CPU processing. Despite great advances in hardware and software in recent years, present computational resources are still insufficient to solve these full core transport problems in a reasonable time (hours-days) that would make the method useful as a design tool. These core calculations are a kind of multiscale problems that are traditionally tackled by solving simpler, smaller problems in specific parts of the core (i.e. cell calculations). Then a procedure known as homogenization is used to create average material properties, and solve the

full problem with a larger mesh size. The fine mesh solution has to be reconstructed afterward using the global shape of the coarse grid solution and the fine structure of the cell calculations.

In this work we present a methodology to solve the transport equation in a fine unstructured grid and correct the fine mesh solution using a multigrid (Trottenberg, 2001) scheme. The multigrid scheme solves the residual equation on a set of coarser structured grids, which reflect the hierarchy of a typical reactor core. This solver was implemented within the framework of the code EVENT (de Oliveira, 1986).

2. Method

2.1. Even parity transport and the code EVENT

Starting from the one-speed transport equation (Eq. 1):

$$\hat{\Omega} \cdot \vec{\nabla} \psi + \sigma \psi =$$
$$\int_{4\pi} d\hat{\Omega}' \sigma_s(\hat{\Omega}' \to \hat{\Omega}) \psi(\vec{r}, \hat{\Omega}') + Q \qquad (1)$$

* Corresponding author, marquezj@ib.cnea.gov.ar
Tel: +54 (2944) 445189, Fax: +54 (2944)445189

we can expand the total cross section and the scattering cross section on Legendre polynomials of $\mu = \hat{\Omega} \cdot \hat{\Omega}'$:

$$\sigma(\vec{r})\psi(\vec{r}, \hat{\Omega}) =$$
$$\sum_{l=0}^{\infty} \frac{2l+1}{4\pi} \sigma(\vec{r}) \int_{4\pi} \mathrm{d}\hat{\Omega}' P_l(\mu_0)\sigma(\vec{r})\psi(\vec{r}, \hat{\Omega}') \qquad (2)$$

$$\int_{4\pi} \mathrm{d}\hat{\Omega}' \sigma_s(\hat{\Omega}' \to \hat{\Omega})\psi(\vec{r}, \hat{\Omega}') =$$
$$\sum_{l=0}^{\infty} \frac{2l+1}{4\pi}\sigma_{sl}(\vec{r}) \int_{4\pi} \mathrm{d}\hat{\Omega}' P_l(\mu_0)\psi(\vec{r}, \hat{\Omega}') \qquad (3)$$
$$\text{with } \sigma_{sl}(\vec{r}) = 2\pi \int_{-1}^{1} \mathrm{d}\mu_0 \sigma(\mu_0) P_l(\mu_0)$$

and rewrite Eq. 1 as:

$$\hat{\Omega} \cdot \vec{\nabla}\psi(\hat{\Omega}) +$$
$$\sum_{l=0}^{\infty} \frac{2l+1}{4\pi}\sigma_l \int_{4\pi} \mathrm{d}\hat{\Omega}' P_l(\mu_0)\psi(\vec{r}, \hat{\Omega}') = Q(\vec{r}, \hat{\Omega}) \qquad (4)$$
$$\text{with } \sigma_l = \sigma - \sigma_{sl}$$

Now, we can separate the even and odd angular components by adding and subtracting Eq. 4 evaluated at $\hat{\Omega}$ and $-\hat{\Omega}$:

$$\hat{\Omega} \cdot \vec{\nabla}\psi^-(\hat{\Omega}) +$$
$$\sum_{\text{even } l} \frac{2l+1}{4\pi}\sigma_l \int_{4\pi} \mathrm{d}\hat{\Omega}' P_l(-\mu_0)\psi^+(\vec{r}, \hat{\Omega}') \qquad (5)$$
$$= Q^-(\vec{r}, \hat{\Omega})$$

$$\hat{\Omega} \cdot \vec{\nabla}\psi^+(\hat{\Omega}) +$$
$$\sum_{\text{odd } l} \frac{2l+1}{4\pi}\sigma_l \int_{4\pi} \mathrm{d}\hat{\Omega}' P_l(-\mu_0)\psi^-(\vec{r}, \hat{\Omega}') \qquad (6)$$
$$= Q^+(\vec{r}, \hat{\Omega})$$

where

$$\psi^\pm = \frac{1}{2}\Big(\psi(\hat{\Omega}) \pm \psi(-\hat{\Omega})\Big) \qquad (7)$$

$$Q^\pm = \frac{1}{2}\Big(Q(\hat{\Omega}) \pm Q(-\hat{\Omega})\Big) \qquad (8)$$

are the even and odd components of the angular flux and the source.

The integral operator on the right hand side of Eq. 6 can be inverted (Ackroyd, 1996) to isolate the even parity flux (ψ^-) and replace it in Eq. 5. The resulting equation (Eq. 9) is the *second order, even parity transport equation*:

$$-\hat{\Omega} \cdot \vec{\nabla}G\hat{\Omega} \cdot \nabla\psi^+ + C\psi^+ =$$
$$Q^+(\vec{r}, \hat{\Omega}) - \hat{\Omega} \cdot \nabla GQ^- \qquad (9)$$

In this equation,

$$Cf(\hat{\Omega}') =$$
$$\sum_{\text{even } l} \frac{2l+1}{4\pi}\sigma_l \int_{4\pi} \mathrm{d}\hat{\Omega}' P_l(-\mu_0)f(\hat{\Omega}') \qquad (10)$$

is the *collision operator* and

$$Gf(\hat{\Omega}') =$$
$$\sum_{\text{odd } l} \frac{2l+1}{4\pi}\sigma_l \int_{4\pi} \mathrm{d}\hat{\Omega}' P_l(-\mu_0)g(\hat{\Omega}') \qquad (11)$$

is the *removal operator*.

EVENT solves Eq. 9 by applying the Ritz-Galerkin procedure using as basis functions the direct product of Lagrange finite elements in space and spherical harmonics in angle (de Oliveira, 1987).

The Ritz-Galerkin procedure creates a system of linear equations which is then solved using standard linear algebra solvers. For each energy group, the coefficient matrix is composed by $M \times M$ blocks of dimension $N \times N$, where M is the number of angular basis functions and N is the number of nodes:

Only the diagonal blocks are explicitly assembled, whereas the non-diagonal blocks are only assembled when the matrix-vector multiplication

routine is called. These diagonal blocks can be interpreted as the coefficient matrix for each moment of the even parity transport equation.

2.2 Multigrid algorithms

The proposed method uses a multigrid algorithm to solve the in-moment equation. The basis for multigrid methods is to take advantage of the spectral properties of stationary iterations, i.e. the smoothing effect of these iterations on the error (Fig. 1).
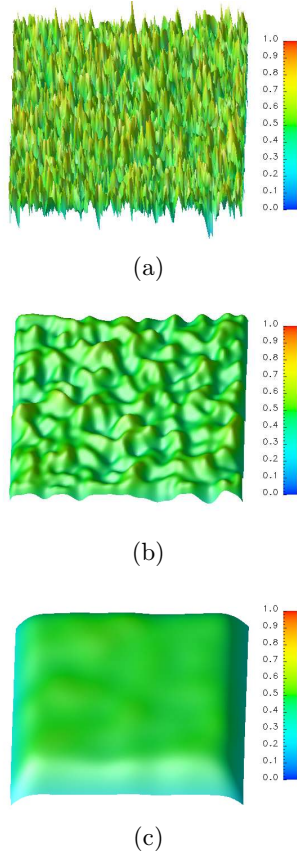
(a)

(b)

(c)

Fig. 1: Effect of (a) one, (b) 10, and (c) 99 point-Jacobi iterations on the error of a homogeneous problem with a random guess.

After a few iterations the change in the error is negligible and the efficiency of the method based on stationary iterations decreases. At this point, multigrid methods compute the residual and project it onto a coarser grid using a restriction operator. In this new grid, an additive correction is sought by solving the error equation:

$$A_c e_c = \mathcal{R}_c^f r \tag{12}$$

where $\mathcal{R}_c^f r$ is the projected residual. In the coarser mesh the error is represented by higher frequency modes, which are attenuated with higher efficiency by the stationary iterations.

After obtaining this additive correction, the solutions is projected back into the fine mesh using an interpolation operator, and then applied to the solution.

$$\mathbf{x}_f^{j+1} = \mathbf{x}_f^j + \mathcal{I}_2^1 \mathbf{e}_c$$

If this method is applied over a set of n meshes each one coarser than the previous, we arrive to the algorithm for a multigrid V-cycle:

- Relax $\mathbf{A}_0 \mathbf{x} = \mathbf{b}$, ν_1 times (ν_1 is usually 1) using the initial value $\mathbf{x}^{(0)}$ as guess.
- Compute the residual: $\mathbf{r}_0^{\nu_1} = \mathbf{b} - \mathbf{A}_0 \mathbf{x}^{(\nu_1)}$.
- Restrict the residual into the next coarse grid: $\mathbf{b}_1 = \mathbf{R}_0^1 \mathbf{r}_0$.
    - Relax $\mathbf{A}_1 \mathbf{x}_1 = \mathbf{b}_1$, ν_1 times using $\mathbf{e}_0^{(0)}$ as initial value.
    - Compute the residual: $\mathbf{r}_1^{\nu_1} = \mathbf{b}_1 - \mathbf{A}_1 \mathbf{x}_1^{(\nu_1)}$.
    - Restrict the residual into the next coarse grid: $\mathbf{b}_2 = \mathcal{R}_1^2 \mathbf{r}_1$.

$$\vdots$$

    - Solve $\mathbf{A}_n \mathbf{x}_n = \mathbf{b}_n$.

$$\vdots$$

    - Interpolate the error and correct the solution: $\mathbf{x}_1^{\nu_1'} = \mathbf{x}_1^{\nu_1} + \mathcal{I}_2^1 \mathbf{x}_2$.
    - Relax $\mathbf{A}_1 \mathbf{x}_1 = \mathbf{b}_1$, ν_2 times (ν_2 is usually 1).
- Interpolate the error and correct the solution: $\mathbf{x}_0^{\nu_1'} = \mathbf{x}_0^{\nu_1} + \mathcal{I}_1^0 \mathbf{x}_1$.
- Relax $\mathbf{A}_0 \mathbf{x}_0 = \mathbf{b}_0$, ν_2 times
- Check the convergence.

3. Implementation

The implementation of the multigrid algorithm required the modification of the EVENT solver

and its preprocessor, GEM. The modifications can be summarized as follows:

1. Meshing and interconnection of different geometrical levels: the preprocessor GEM was modified to allow meshing of multi-level problems.

   The finest mesh was allowed to be unstructured, whereas the second to n-th mesh are structured (Fig. 2). This way, the fine mesh can be used to define the details of a typical fuel-pin cell, and the coarser mesh can be used to represent the cell, assembly and core levels of a reactor
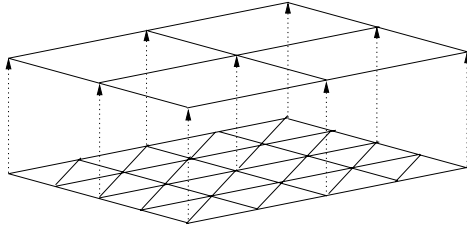

Fig. 2. First (unstructured) and second (structured) meshes.

   To simplify the implementation, the interconnection between levels was based on geometrical superposition. Each point on a coarse mesh was forced to exist in all the finer meshes.

2. Assembly of coarse grid coefficient matrices: volume weighted homogenization routines were introduced to the preprocessor GEM to generate the material properties for the coarse levels. The coarse grid coefficient matrices are then assembled using the existing EVENT routines.

3. Calculation of the restriction and interpolation operators to communicate the levels: a subroutine to compute the restriction and interpolation operators was implemented in EVENT. This subroutine is called once, at the beginning of a multigrid calculation. The coefficients

for the restriction $(\mathcal{R}_c^f)$ operator are computed by the evaluation of the coarse mesh basis function on the fine mesh nodes inscribed in the coarse mesh element (Fig. 3).
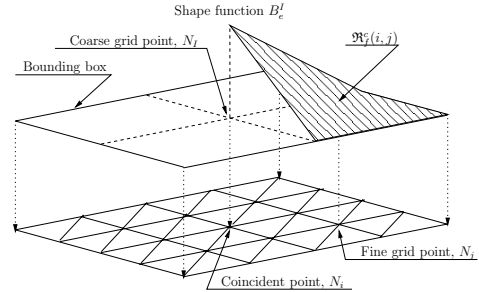

Fig. 3. Scheme of the computation of coefficients for the restriction operator.

The interpolation operator $(\mathcal{I}_f^c)$ is the restriction operator matrix, transposed and scaled.

4. Iterative sweep to relax the solution: point Jacobi and Gauss-Seidel iterations were implemented to be used either as a standalone iterative solver, or as part of a multigrid V-cycle.

5. An exact solver to find the correction on the coarser grid: in order to solve the error equation in the coarser grid, a Gauss-Jordan matrix inverting routine was implemented as part of the multigrid solver.

4. Results

4.1 Computational cost analysis

The multigrid solver was tested against the standard EVENT solver, which uses the preconditioned conjugate gradients method. EVENT has been validated using analytical solutions and experimental benchmarks (Keller and de Oliveira, 2004; Park, 2006).

A simple diffusion problem (Figure 1a) was used to estimate the savings in computational

4

costs yielded by the algorithm. The results show a reduction in computer time (Figure 1b) both in magnitude and in the order it scales with the number of nodes.
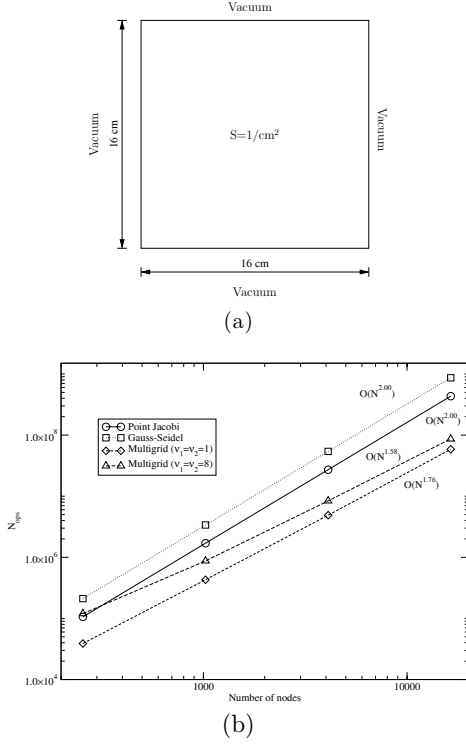

(a)

(b)

Fig. 4: Comparison of computational cost (b) for a one-group, uniform source diffusion problem (a).

4.2 Transport solver test

The transport solver was tested with a four region problem with diagonal symmetry (Figure 2a). Lower left quarters has a strong absorbing material, whereas in the other three the scattering is prevalent. In the upper left quarter there is a source, which creates a gradient in the neutron flux. The system is surrounded by vacuum boundary conditions.

The problem was solved using P_3 expansion of the even parity flux (Fig. 2b). The solution shows the solver preserve the symmetry of the problem and the smoothness is not affected by the coarse mesh linear correction. The solution was compared (Fig. 2c) with a reference solution obtained with the conjugate gradient solver in EVENT, using a tolerance two orders of magnitude higher. The difference in the solution is less than the tolerance used in multigrid calculations ($\varepsilon = 10^{-4}$).
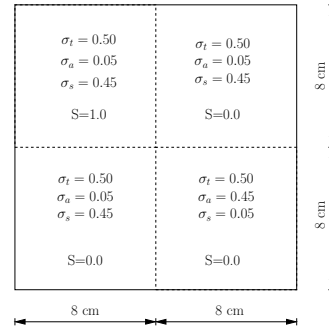

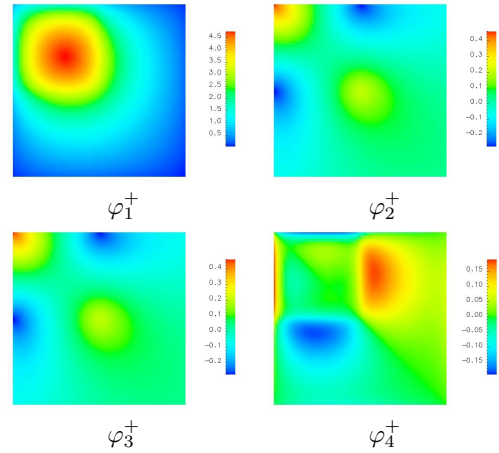Fig. 5: Transport test problem. a) Geometry and material distribution.

Fig. 6: Transport test problem. a) Geometry and material distribution.

5

$$\varphi_1^+ - \varphi_{1,\,\mathrm{ref}}^+ \qquad\qquad \varphi_2^+ - \varphi_{2,\,\mathrm{ref}}^+$$

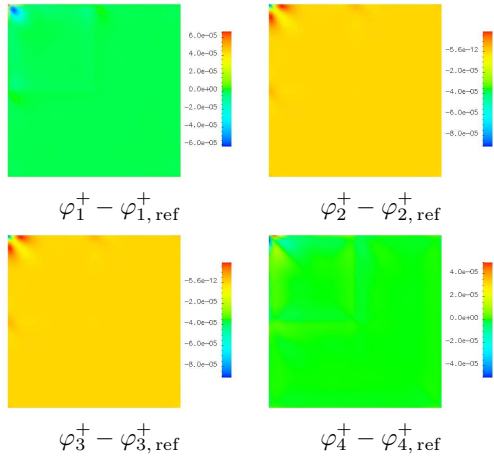$$\varphi_3^+ - \varphi_{3,\,\mathrm{ref}}^+ \qquad\qquad \varphi_4^+ - \varphi_{4,\,\mathrm{ref}}^+$$

Fig. 7: Transport test problem. a) Geometry and material distribution.

4.3 Solver test with unstructured grids

To test the solver with an unstructured grid on a real problem, a 17×17 UO_2 fuel pin PWR assembly (Fig. 8), taken from the C5G7 MOX benchmark specification (Lewis et al, 2001) was solved. The geometry was discretized using $h \simeq 0.25$cm (5 elements per cell side, 4 elements per pin quadrant), resulting in a 10864 nodes fine mesh. A reference solution was obtained using the EVENT preconditioned conjugate gradient solver, resulting in a multiplication factor $k_{eff} = 1.33737$.
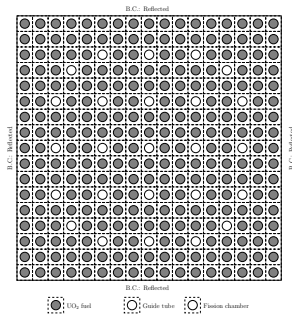

Fig. 8: Transport test problem. a) Geometry and material distribution.

$$\phi_1 \qquad\qquad \phi_2$$

$$\phi_3 \qquad\qquad \phi_4$$
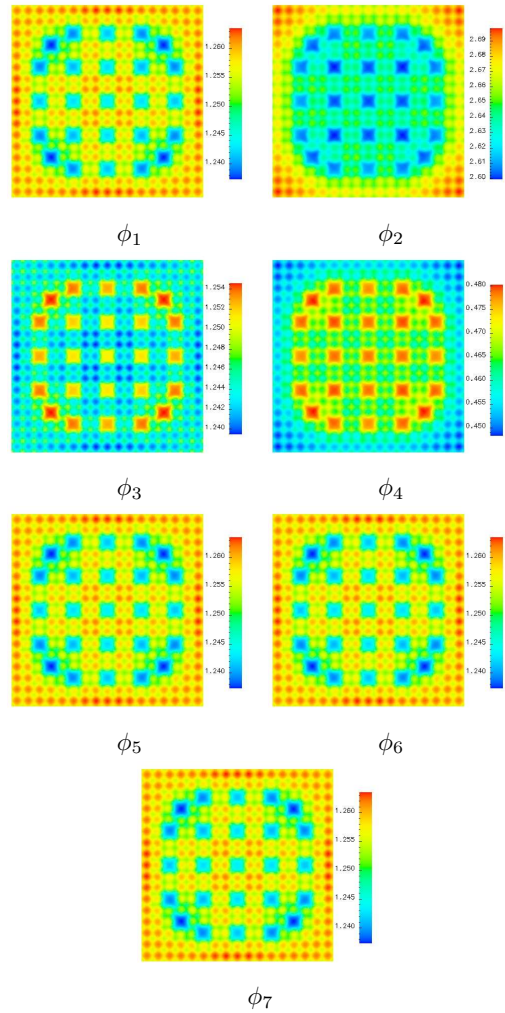
$$\phi_5 \qquad\qquad \phi_6$$

$$\phi_7$$

Fig. 9: Transport test problem. a) Geometry and material distribution.

The unaccelerated solvers needed 417992 (Jacobi) and 210832 (Gauss-Seidel) relaxation iterations to converge to the desired tolerance. The multigrid solver was run with a three level structure with 18×18 nodes and 9×9 nodes in the coarse levels, converging in 94528 relaxation iterations.

The scalar flux maps for each group (Fig. 9)

show the shift in maximum flux from the center of the fuel pins to the moderator that surrounds the pins and fills the guide tubes.

Additional numerical results were obtained (Marquez Damian, 2007), but are omitted here for brevity.

5. Conclusions

A proof of concept multigrid solver for the even parity second order transport equation has been implemented using the infrastructure provided by the finite element, spherical harmonics code EVENT. The solver was implemented for the solution of the diffusion-like in-moment equation and a block Jacobi scheme was used to update the residual in higher order problems. The solver was tested satisfactorily for the solution of the diffusion and transport equation with fixed sources and for eigenvalue problems.

The results show the implemented multilevel scheme outperformed the direct application of the relaxation iterations, both in total computational cost and in the order on which the cost scales with the number of nodes. This difference is more important for optically thin, highly scattering (diffusive) problems where the one-level solver convergence is particularly low.

The rather simple relaxation iteration and coarse grid solver used limited the overall efficiency of the method, which still could not be compared to the highly optimized preconditioned conjugate gradient solver already implemented in the code. Nevertheless, the positive results obtained with these simple tools made interesting the research on the combination of a hybrid method, either using multigrid as a preconditioner for the conjugate gradient solver or using the conjugate gradient method for the coarse grid solver.

References

de Oliveira, C.R.E., An arbitrary geometry finite element method for multigroup neutron transport with anisotropic scattering, Prog. Nucl. Energy, vol. 18, no. 1/2, pp. 227-236, 1986.

de Oliveira, C.R.E., Finite element techniques for multi-group neutron transport calculations with anisotropic scattering. PhD Thesis, Queen Mary College, University of London, UK, 1987.

Keller, S.E., de Oliveira, C.R.E., Two-Dimensional C5G7 Mox Fuel Assembly Benchmark Calculations Using the FEM-PN Code EVENT, Prog. In Nuclear Energy, vol. 45, p. 255, 2004.

Lewis, E.E., Benchmark specification for Deterministic 2-D/3-D MOX fuel assembly transport calculations without spatial homogenization (C5G7 MOX), tech. rep NEA/NSC/DOC, 2001.

Marquez Damian, J.I., Multilevel acceleration of neutron transport calculations. MSc thesis, Georgia Institute of Technology, Atlanta, GA, 2007.

Park, H.K., Coupled Space-Angle Adaptivity and Goal-Oriented Error Control for Radiation Transport Calculations. PhD thesis, Georgia Institute of Technology, Atlanta, GA, 2006.

Trottenberg, U., Oosterlee, C.W., Multigrid. Academic Press, 2001.